Effect of Pulse Current on Interface Microstructure and Bonding Properties of TA1/304 Double-Layer Clad plates

Xiongwei Guo[1,2,3,4], Zhongkai Ren[1,2,3,4*], Pengjie Zhang[1,2,3,4], Chao Zhang[1,2,3,4], Shuyong Jiang[2,3,4], Qi Zhang[1,2,3,4*], Tao Wang[1,2,3,4] and Qingxue Huang[1,2,3,4]

Abstract

It is difficult to effectively improve the low bonding strength of TA1/304 clad plates. This study proposes a new process for applying pulse current (1500 A, 500 Hz, 50% duty cycle) to TA1/304 clad plates during the rolling process, which changes the interface microstructure and effectively improves the bonding strength of the clad plates. The influence of the pulsed current on the interface microstructure and bonding strength was systematically studied. The results indicate that the clad plate is initially bonded at 750 °C and 35% reduction ratio under electrically-assisted rolling (EAR), and finally the higher bonding strength is obtained at 850 °C and 48% reduction ratio, reaching 395 MPa. The strengthening of the interface element diffusion and grain refinement under the action of the pulsed current are important reasons for the improvement in the bonding strength of the clad plate. This discovery provides new ideas for the preparation of clad plates with high bonding performance.

Keywords TA1/304 clad plates, Electrically-assisted rolling (EAR), Element diffusion, Microstructure, Tensile shear strength

1 Introduction

Titanium/steel clad plate exhibits the excellent corrosion resistance of titanium and the good mechanical properties of steel. It has important applications in marine engineering, aerospace, petrochemicals, and other fields. Researchers have explored a variety of techniques for preparing high-performance titanium/steel clad plates. Among them, the rolling process has high production efficiency, safety, and stability and is expected to become the mainstream process for the preparation of titanium/steel clad plates in future industrial production.

At present, owing to the significant differences in the physical properties and metallurgical incompatibility between titanium and steel, there is a problem of deformation incompatibility during rolling. Large residual stresses and brittle intermetallic compounds are generated at the interface, resulting in relatively low bonding strength between titanium and steel. Therefore, researchers have primarily focused on adjusting the rolling process to improve the interfacial bonding strength of titanium/steel clad plates. Changing the reduction ratio and rolling temperature are the two most important methods. It is found that breaking the metal oxide film can be achieved by increasing the reduction ratio, and the hard and brittle precipitates such as TiC formed

*Correspondence:
Zhongkai Ren
zhongkai_0808@126.com
Qi Zhang
zhangqi01@tyut.edu.cn
[1] College of Mechanical and Vehicle Engineering, Taiyuan University of Technology, Taiyuan 030024, China
[2] Engineering Research Center of Advanced Metal Composites Forming Technology and Equipment, Ministry of Education, Taiyuan University of Technology, Taiyuan 030024, China
[3] National Key Laboratory of Metal Forming Technology and Heavy Equipment, Taiyuan 030024, China
[4] China-Australia Joint Research Center of Taiyuan University of Technology, Taiyuan 030024, China

at the interface can be broken and dispersed to enhance the interface bonding strength [1]. However, it is difficult to ensure the coordinated deformation of the two metals under a high first pass reduction ratio, which makes the clad plate micro-crack expand, and the allowable rolling force of the rolling mill is put forward higher requirements.

Controlling the bonding strength of titanium/steel clad plates using temperature has become a popular research topic. Zhao et al. [2] studied the effect of temperature on the mechanical properties of cold spray-assisted hot-rolled titanium/steel clad plates in the range of 850–1050 °C. The results showed that the bonding strength decreased significantly with the increase of temperature above 950 °C. At the same time, it was proved that brittle compounds (Fe-Ti, TiC) control the properties of titanium/steel clad plates, and the 4 μm thick diffusion layer exhibits poor mechanical properties at 1050 °C. Yu et al. [3] combined TA2 and Q235B by rolling at 850 °C, and the shear strength reached 271.2 MPa at a 68% reduction ratio. However, the interface shear strength of TA2/Q235B clad plates prepared at 950 and 1050 °C decreased significantly, which was due to the formation of brittle compounds of Fe-Ti and TiC in the ferrite region near the interface at higher temperatures. It can be seen that the bonding performance of the clad plate is improved by adjusting the rolling temperature, but high temperatures caused the interface compound to grow too fast, easily causing cracks and spontaneous expansion, resulting in the failure of the clad plate, especially when the temperature is higher than the phase transition point of α-Ti [4].

In recent years, the concept of electrically assisted processing (EAP) has been proposed, which is considered a promising processing technology, and has gradually become an important development direction in the field of metal forming manufacturing. Researchers have attempted to introduce a pulsed current into the rolling process of a single material and achieved good results. Xu et al. [5] found that an AZ31 strip produced by electroplastic rolling (ER) has a lower deformation resistance and better toughness. Kuang et al. [6] carried out single-pass large-strain electroplastic rolling (LSER) of an AZ31 alloy with different pulsed current densities. They believe that the nonthermal effect of the pulse current on the deformation mechanism makes LSER an effective texture modification technology for magnesium alloys, which can improve formability. In recent years, pulsed current has been applied in the preparation of dissimilar metal composite plates to obtain better bonding properties. However, there are few related studies, and the content of this study is relatively simple. Guo et al. [7] first studied the effect of a pulse current on the bonding strength during the rolling process of composite plates, then explored the influence of a pulse current on the bonding strength of composite plates at different temperatures and reduction ratios. This study did not further investigate the effect of the pulse current on the matrix microstructure. Zhang et al. [8] applied pulse current-assisted rolling welding (PCARW) technology to manufacture Mg/Al alloy plates and found that metal droplets were formed at the interface at high temperatures and squeezed during rolling, resulting in a serrated morphology in the interface transition layer. However, there is a lack of research on the microstructure. Ren et al. [9] studied the effects of current density and annealing time on the mechanical properties of TA1/304 stainless steel-clad plates by pulse-current post-treatment. The best mechanical properties were obtained when the current density was 25.3 A/mm^2 and the time was 1 min. However, systematic and in-depth research on electrically assisted rolling (EAR) is lacking, and its internal mechanism requires further study. For example, the influence of microstructure on the diffusion of interface elements, matrix strength, and interface bonding strength is very important. It is necessary to analyze the contribution of current to the diffusion of interface elements and dislocation motion in combination with the microstructure, using a method such as electron backscatter diffractometry (EBSD).

This paper proposes a new hot-rolling process for titanium/steel clad plates. Using a modified rolling mill, a pulsed current was completely applied to the titanium/steel plates of the asymmetric billet during the rolling process. Then, in the temperature range of 750–900 °C, EAR tests with reduction rates of 35% and 48% were carried out, with current parameters of 500 A, 1500 Hz and 50% duty cycle. The effects of the pulsed current on the interface microstructure and shear strength of the clad plates were systematically analyzed. The internal mechanism of the improvement in the interface bonding strength of the clad plates under the action of pulsed current was revealed.
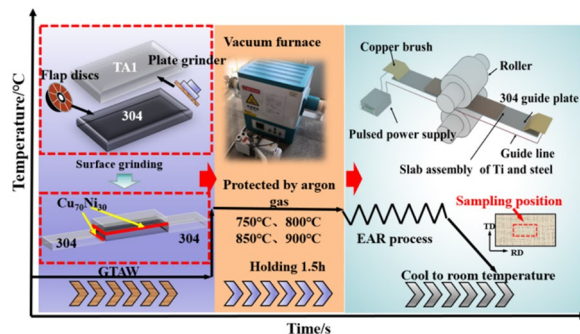
2 Materials and Methods
2.1 Materials
Commercial-grade pure Ti (TA1) and 304 stainless steel were used as raw materials; their chemical compositions are listed in Table 1. The TA1 was 100 × 60 × 2 mm, and the sizes of the 304 stainless steels were 120 × 60 × 3 mm and 140 × 60 × 1 mm. The 3 mm thick steel was used to form billets with TA1, and the 1 mm thick steel was used to connect the copper brush. The 3 mm thick 304 stainless steel was longer than the TA1 to avoid cracking caused by secondary welding during the subsequent billet assembly process.

Guo *et al. Chinese Journal of Mechanical Engineering* (2024) 37:116

Page 3 of 16

Table 1 Chemical composition of 304 stainless steel and TA1 (w.t.%)

Materials	C	Si	Mn	P	S	Ni	Fe	Cr	Cu	Ti
304	0.052	0.36	0.89	0.032	0.002	8.083	Bal.	18.089	0.155	0.008
TA1	—	—	—	—	—	—	0.03	—	—	Bal.

Figure 1 The schematic diagram of the composite plate rolling compound process

Figure 2 Rolling mill modifications: **a** The entrance of rolling mill, **b** The exit of rolling mill, **c** The front of the slab after assembly, **d** The flank of the slab after assembly

2.2 Test Method and EAR Equipment Introduction

Figure 1 shows a flowchart of the billet and rolling process. Before assembly, the surfaces of the 304 and TA1 plates were polished with a flap disc and plate grinder to remove metal surface oxide, repeatedly cleaned with alcohol, and immediately dried. The treated plates were stacked in double layers, and a Cu70Ni30 welding wire was used to perform gas tungsten arc welding (GTAW) with an 80 A welding current under argon gas to achieve a double-layer plate assembly. A 304 stainless-steel plate with dimensions of $140 \times 60 \times 1$ mm was welded on both sides of the stainless steel to facilitate the application of a pulse current. Then the prepared billets were put into the heating furnace at a gradient interval of 50 °C at 750–900 °C for 1.5 h, shielded by argon gas. Subsequently, the heated blank was pushed into the fixture for pulse current-assisted rolling. The current parameters in the rolling process were set to 500 A, 1500 Hz and 50% duty cycles. Through single-pass hot rolling, the reduction ratios reached 35% and 48%, and the rolling speed was 0.12 m/s. Finally, all the clad plates were cooled to room temperature.

The rolling mill required modification to ensure that the pulse current flows through the rolling zone completely during the rolling process. As shown in Figure 2, pulse-current application fixtures were set at the entrance and exit of the rolling mill (Figure 2a, b), and the current was applied through the contact between the copper brush and the slab. Simultaneously, the contact part between the fixture and frame was connected to the insulating screw through the insulating plate, which

not only ensured the safety of the experiment, but also reduced the current loss during the experiment as much as possible. The elongated 304 stainless-steel guide plate ensured that the billet (Figure 2c, d) was rolled with the assistance of a pulse current throughout the rolling process.

2.3 Tensile Shear Test and Microstructure Characterization

The samples used for the tensile-shear test and microstructure characterization were prepared using wire electrical discharge machining along the rolling direction of the plate. The shear strength was calculated by $\tau = F/S$, where τ was the strength (MPa), F was the loading force (N), S was the lap area (mm²), and the tensile shear specimen was shown in Figure 3. An Instron Series 5969 testing machine (Instron Ltd., Norwood, MA, USA) was used at room temperature at a pull rate of 1 mm/min. Three samples from each condition were tested to ensure the repeatability of the results.

The interface characteristics of the samples were observed using a scanning electron microscope (SEM, JOEIT500, JEOL Ltd., Tokyo, Japan) equipped with an energy dispersive spectrometer (EDS) and EBSD. The samples for microstructural observation were ground with emery papers up to No. 2000 and polished with a SiO_2 suspension having a particle size of 0.04 μm. The EBSD samples were initially polished for 1 h with a 2.5 kV ion beam on a Leica RES101 (Leica, Wetzlar, Germany).

Guo *et al. Chinese Journal of Mechanical Engineering*   (2024) 37:116
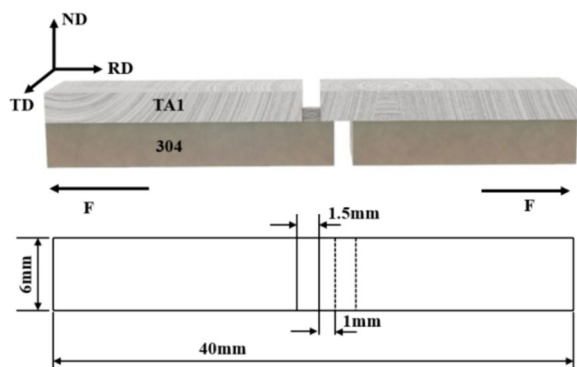
Page 4 of 16

Figure 3 The schematic diagram of the samples for the tensile shear test

At 20 kV and 0.5 μm steps, the corresponding EBSD data were obtained by SEM, and then the data were analyzed by Channel 5 and Aztec Crystal software.

3 Results

3.1 Interface Structure

Figure 4a–d shows the SEM images of the interface at a 35% reduction ratio. The thickness of the TA1 layer was measured under different rolling conditions, and the ratio of the TA1 layer thickness to the total thickness was calculated. The statistical results are shown in Figure 5. The thickness of the TA1 layer accounts for about 41% under different working conditions. Evidently, the EAR did not significantly change the thickness ratio of the TA1/304 clad plates. Figure 4e–h shows the scan routes of the interface. When the temperature is 800 °C, the conventional rolling (CR) interface element diffusion is about 1.3 μm, and the EAR interface increases to 1.6 μm. At 850 °C, the element diffusion at the CR interface is about 1.7 μm, and the EAR interface increases to 2.0 μm (Figure 4i–l EDS line scan results). Therefore, the EDS results show that the EAR leads to a more intense diffusion of elements.

3.2 Microstructure Evolution

It is not difficult to see that there are significant differences in element diffusion in Figure 4, and this difference is mainly due to the change in the matrix microstructure. Therefore, microstructural analysis of the steel-side matrix is helpful for understanding the influence mechanism of the current on the microstructure and element diffusion. Therefore, EBSD analysis was first performed on steel near the interface at a 35% reduction ratio. The sampling position is shown
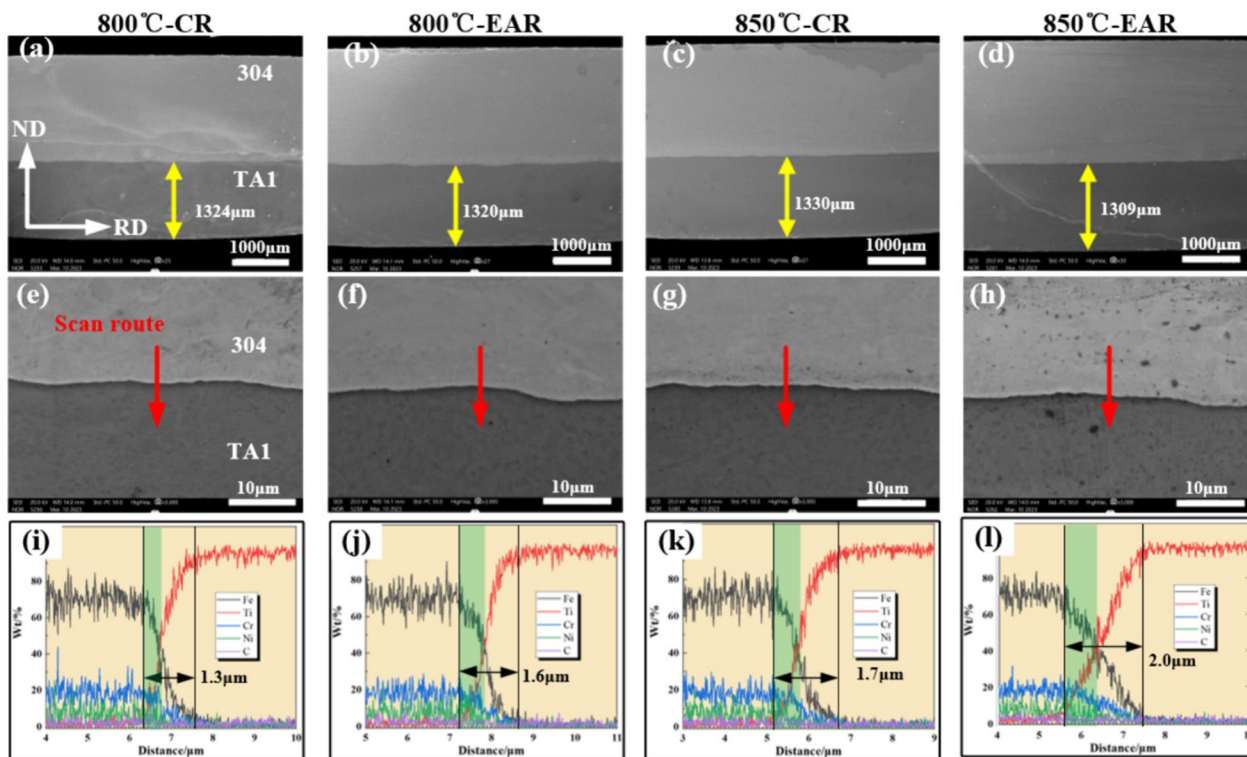

Figure 4 a–h The SEM images of the clad interface with a reduction ratio of 35%, **i–l** EDS line scan curves corresponding to red lines segment marked in panels (**e–h**)
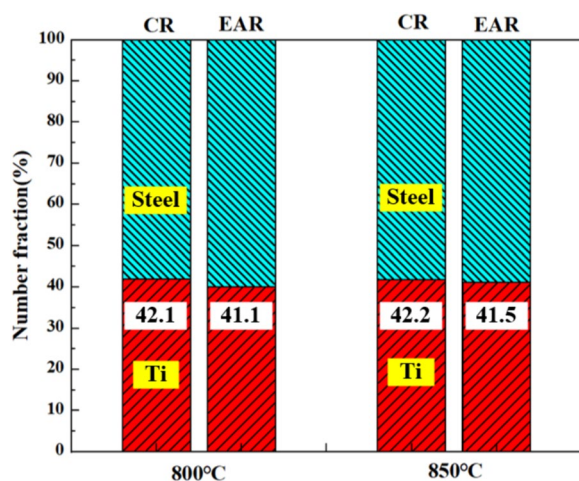
Figure 5 Statistics of the thickness proportion of each layer of Ti/ steel clad plates at the reduction ratio of 35%
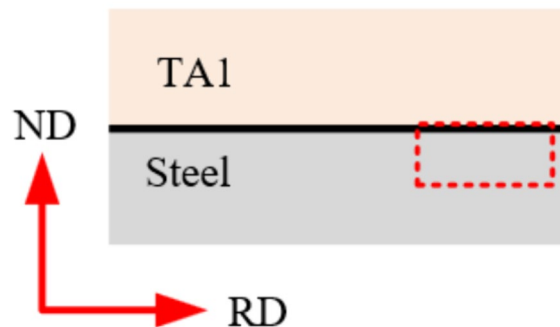

Figure 6 EBSD sampling location

in Figure 6. Figure 7 shows the EBSD results, including the grain size maps (a–d), kernel average misorientation (KAM) maps (e–h), and grain boundary distributions (i–l) of the TA1/ 304 plates under different conditions. As shown in Figure 7a–d, when plastic deformation occurs, the geometry and orientation of the grains change, resulting in uneven grain orientation. After rolling deformation, the grains are elongated and more obvious at 850 ℃.

The KAM diagrams in Figure 7e–h reflect the distribution and difference in the local strain in the microstructure. KAM is also useful for calculating the geometrically necessary dislocation (GND) density in crystalline materials, and reflects the local dislocation density of the material. The higher the value, the greater the degree of local plastic deformation and the higher the dislocation density of the material [10]. A large number of local strains caused by rolling deformation are observed on the stainless steel side after rolling, and the average KAM increases from 0.94 ° to 1.11° at EAR and 800 ℃. At 850 ℃, the average KAM increases from 1.06° to 1.41°. Overall, the local strain distribution under the CR condition was not uniform, the local strain under the EAR condition was significantly improved, and the uniformity of the dislocation distribution was improved.

Figure 7i–l shows the distribution maps of the low-angle grain boundaries (LAGBs) and high-angle grain boundaries (HAGBs). Among them, the part with grain boundary misorientation of 2°–15° was defined as LAGB, and the part with grain boundary misorientation greater than 15° was defined as HAGB. It can be observed from the figure that at the same temperature, the LAGBs on the steel side under EAR conditions increased significantly. When the rolling temperature was 800 ℃,

the proportion of LAGB in the 304 stainless steel layer under the action of pulse current increased from 46.6% to 52.2%, and the average orientation difference decreased from 40.70° to 38.74°. When the rolling temperature is 850 ℃, the proportion of LAGBs in the stainless steel layer increased from 59.4% to 70.7%, and the average grain boundary misorientation decreased from 36.49° to 32.57°. The statistical results are shown in Figure 8c–d.

Figure 9 shows the EBSD results near the interface after conventional rolling and pulse current assisted rolling at 850 ℃ and a 35 % reduction ratio. As shown in Figure 9a, d, the interface after rolling showed good bonding quality without pores or cracks, but the grain size on both sides of the interface changed significantly. The grain size of the TA1 side after CR was 5.07 μm, and the grain size of the TA1 side after EAR was 8.52 μm. In addition, the grain distribution was not uniform near the interface after EAR, and obvious shear bands and a large number of fine-grained zones were observed. The grain deformation on the steel side after EAR was larger, showing an elongated state, and the grain size was 25.4 μm, which is significantly smaller than the 32.2 μm of CR. It can be seen that the effect of current on the grain refinement of the matrix is significant.

To clarify the distribution of dislocations in the TA1/304 clad plates after EAR, the KAM method was used to calculate the local misorientation on both sides of the interface from the EBSD data (Figure 10). For calculating local misorientation, the range of grain boundary misorientation was limited to less than 2°, because the misorientation of grain boundaries greater than 2° was caused by grain boundaries, not by GND pile-up. The strain gradient theory established by Gao et al. [11] and Kubin et al. [12] was used to calculate GND density.

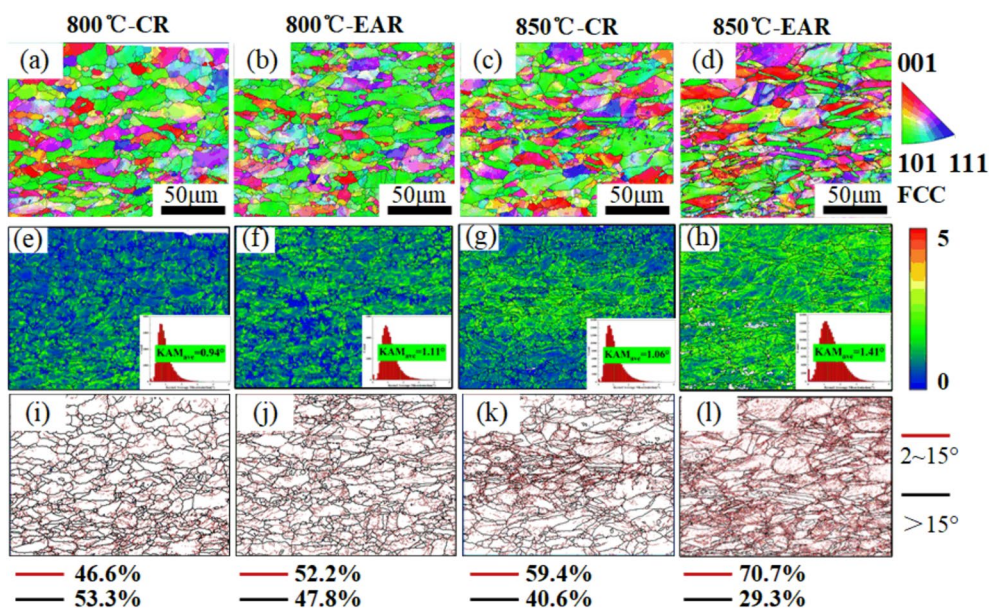$$\rho^{GND} = \frac{2\theta}{\mu b}, \tag{1}$$

Figure 7 EBSD results of the 304 said at interface: **a**–**d** grain size maps, **e**–**h** KAM maps, **i**–**l** grain boundary distributions

where ρ is the GND density, θ is the local misorientation, b is the Burgers vector, μ is the scanning step (0.5 μm). The calculation results for the GND density near the TA1/304 clad plate interface under CR and EAR conditions are shown in Figure 9c, f, respectively. It can be seen that the GND density near the interface under different rolling processes is significantly different, and the GND density on the steel side under EAR is obviously higher than that under CR.

Figure 11 shows the average GND density statistics of the matrix on both sides under different working conditions. The GND density of the steel layer under EAR (5.84×1014 m^{-2}) was higher than that under CR (4.94×1014 m^{-2}). In contrast, the GND density of the TA1 layer under the EAR (4.67×1014 m^{-2}) was lower than that under the CR (5.41×1014 m^{-2}). From these results, it can be observed that there was a difference between the strengthening of the TA1 and 304 layers during the EAR process. The increase in the interface deformation led to grain refinement on the TA1 side and an increase in the dislocation density on the 304 side.

Figure 12 illustrates the distribution of recrystallized, sub-structured, and large deformed grains. On the TA1 side of CR, the proportion of deformed grains was 37.08% and the recrystallized grains were evenly distributed throughout the TA1 layer (Figure 12a). Compared to CR, the proportion of deformed grains on the TA1 side under EAR was reduced to 27.45%, and the recrystallized

grains were concentrated in the fine grain region near the interface (Figure 12d). In contrast to TA1, the proportion of deformed grains on the 304 side at CR was 42.23%, and the proportion of deformed grains at EAR increased to 69.37%.

3.3 Mechanical Property

The tensile-shear properties of the TA1/304 clad plates were tested under different working conditions, and the results are shown in Figure 13. Figure 13a shows the tensile shear curve for a 35% reduction under different rolling conditions. The clad plate was initially combined at 750 °C under EAR, but the shear strength was only 113 MPa. As the rolling temperature increased, the shear strength increased significantly. At 800 °C, the shear strengths were 260 MPa under CR and 287 MPa under EAR. At 850 °C, the shear strengths were 297 MPa under CR and 338 MPa under EAR.

Figure 13b shows the tensile shear curves at 48% reduction under different rolling conditions. The tensile shear strength increased with the reduction ratio. The bonding strength of the clad plate is significantly improved at 750 °C under EAR, reaching 179 MPa. Increasing the temperature remains an effective way to improve the bonding strength. The shear strength increased from 327 MPa to 36 8MPa under CR at 800 °C and from 319 MPa to 395 MPa under EAR. However, the tensile shear strength decreased when the temperature reached 900
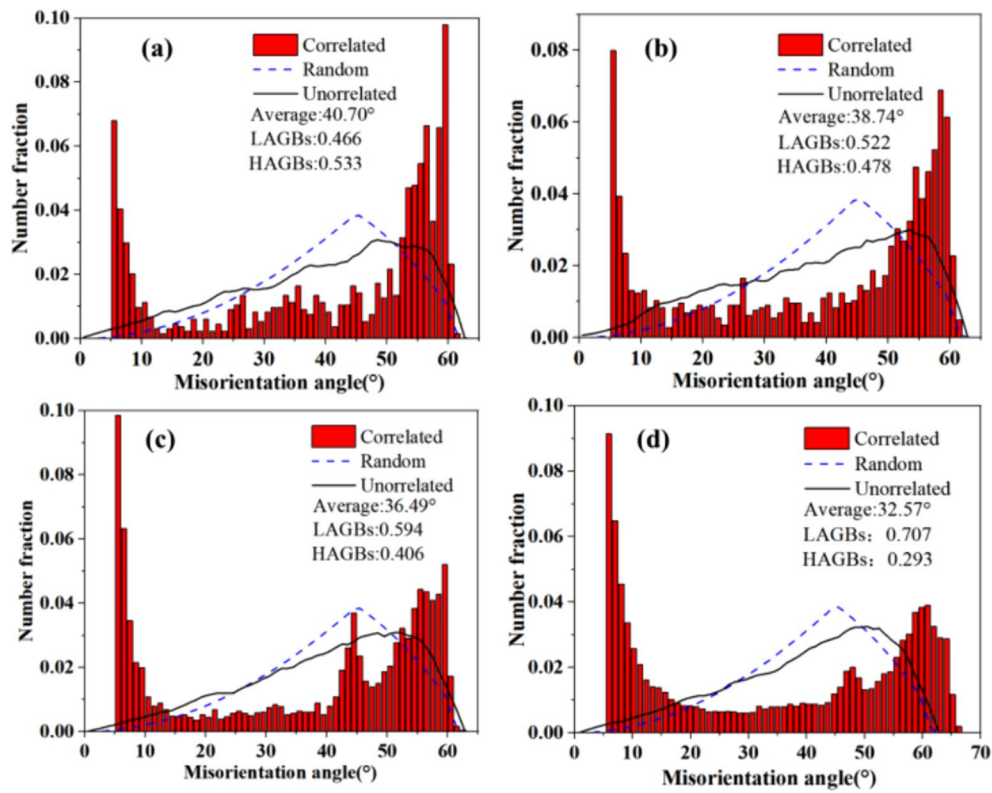
Figure 8 Misorientation angle distribution maps of 304 stainless steel at 35% reduction ratio: **a** 800℃-CR, **b** 800℃-EAR, **c** 850℃-CR, **d** 850℃-EAR
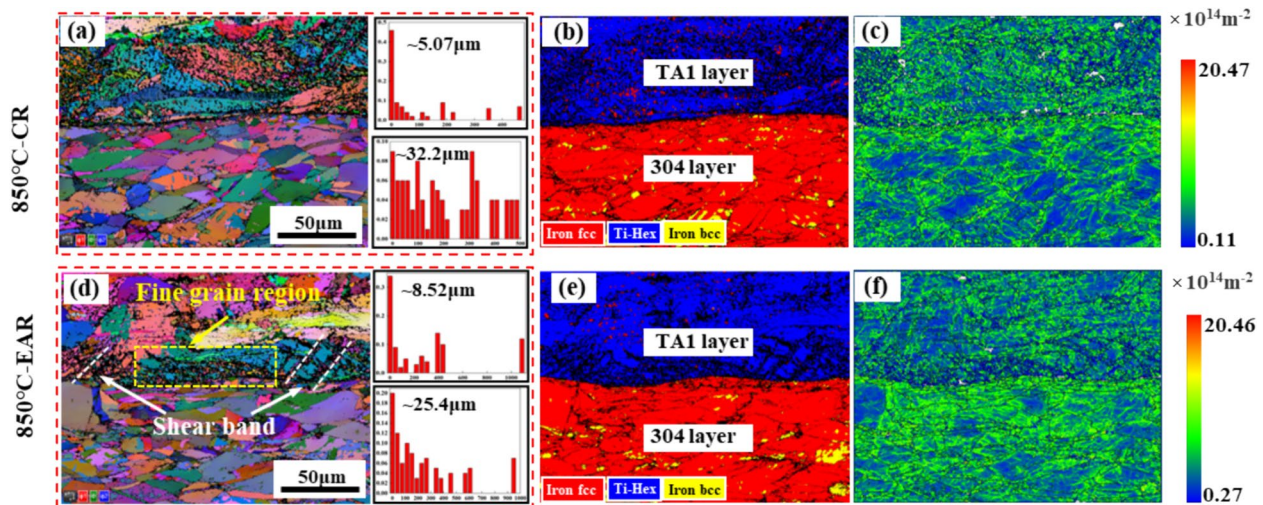

Figure 9 EBSD result of the TA1/304 clad plates at interface: **a**, **d** grain size maps and histogram; **b**, **e** phase maps; (**c**), **f** GND distributions

°C, yielding at 225 MPa and 284 MPa under CR and EAR conditions, respectively.

Figure 13c shows the typical tensile-shear fracture characteristics of the TA1/304 clad plates under different conditions. Under the condition of 750 °C-35%-EAR, the fracture surface was parallel to the rolling direction (RD).

Under the condition of 850 °C-35%-EAR, the fracture was 15° to the RD, and under the condition of 850 °C -48 %-EAR, the fracture was 21° to the RD. Overall, the shear properties of TA1/304 clad plates were improved under the action of pulse current below 850 °C, and the shear
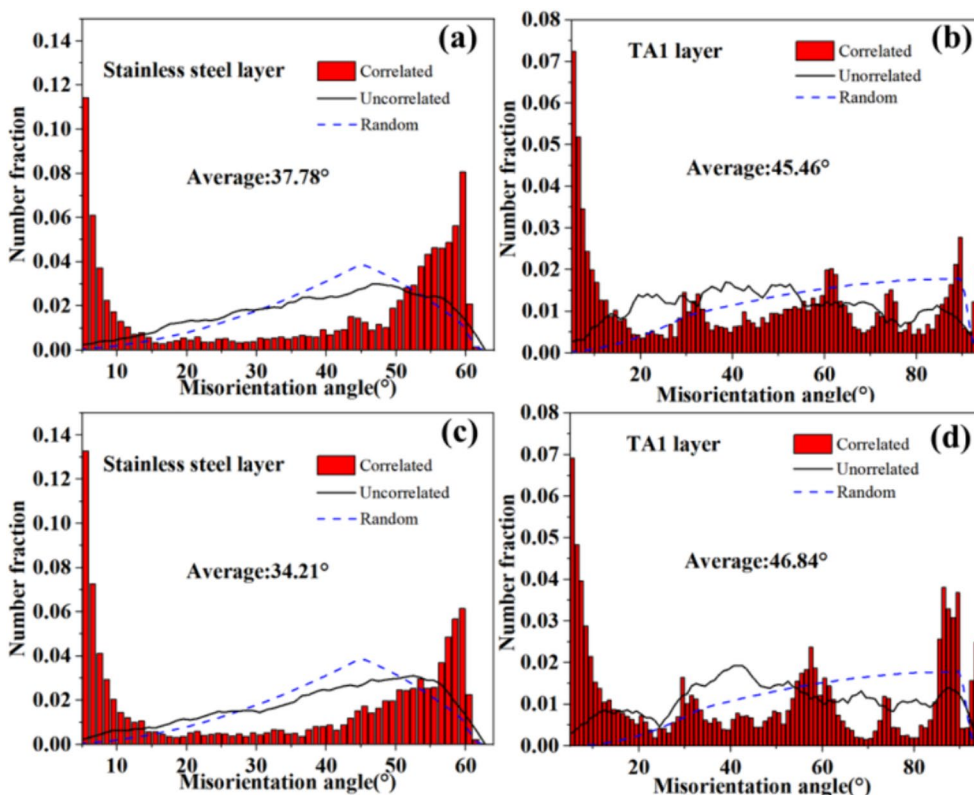
Figure 10 Misorientation angle distribution maps of TA1/304 clad plates at 850℃: (**a**), (**b**) CR, (**c**), (**d**)EAR
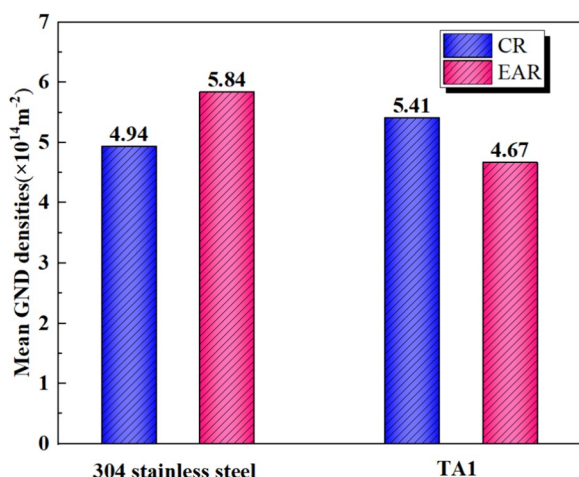

Figure 11 The mean GND densities in TA1 and 304 stainless steel layers

strength began to decrease when the rolling temperature was higher than 850 ℃.

3.4 Fracture Morphology

Figure 14 shows the experimental results and fracture morphologies under different rolling conditions at 750 ℃. As shown in Figure 14a, when the reduction ratio was 35%, the interface between TA1 and 304 under CR showed obvious cracking and no bonding, while under EAR, the interface between TA1 and 304 was obviously bonded. Figure 14b−d shows the shear section morphology and surface scanning results under a 35% reduction ratio and EAR conditions. The fracture surface exhibited a small amount of island matrix residue. Surface scanning results showed that the residue was a TA1 matrix. After the reduction ratio was increased to 48%, the SEM morphology showed that a large amount of TA1 matrix tearing remained on the steel side (Figure 14e−g), suggesting an increased bond strength.

Figure 15 shows the shear fracture morphology of the steel side under different rolling conditions at 800 ℃. When the reduction ratio was 35%, there was a small amount of island TA1 matrix residue on the steel side of the shear fracture under CR conditions. Under the EAR condition, a large area of TA1 matrix tearing remained in the shear section. When the reduction ratio was increased to 48% in the CR process, there was a large area of TA1 matrix tearing residue in the lower section, and dimples were found on the TA1 matrix. Similarly, the coverage area of the TA1 matrix increased under EAR conditions. In general, the shear fracture of TA1/304 clad
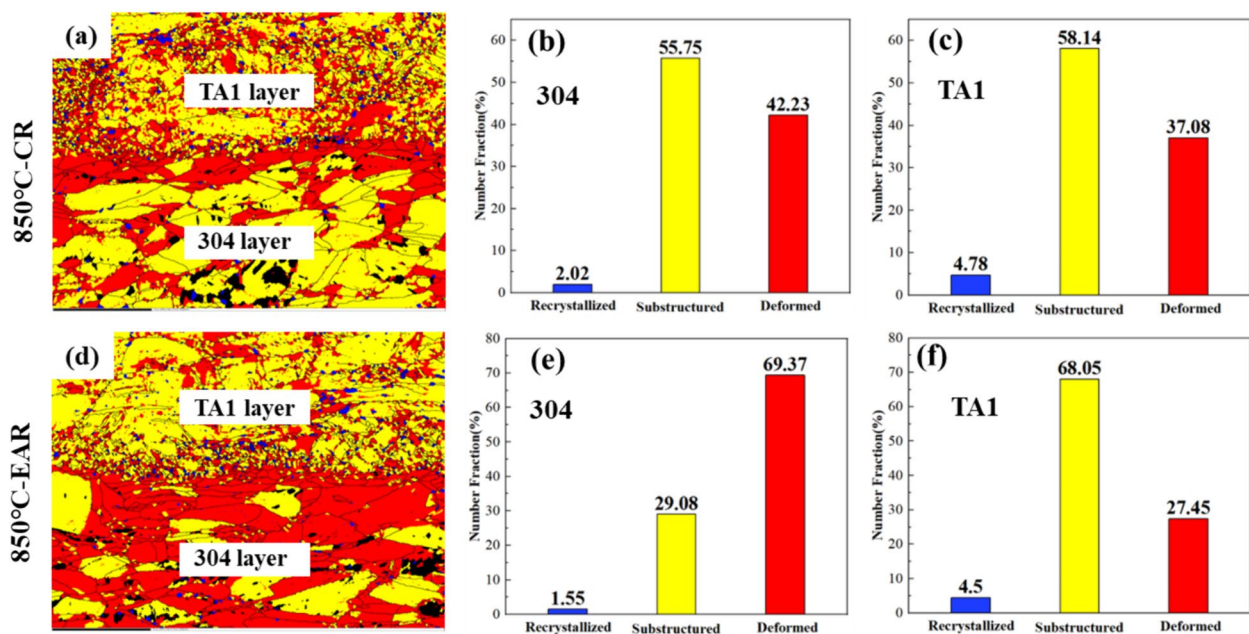
Guo *et al. Chinese Journal of Mechanical Engineering* (2024) 37:116

Page 9 of 16

Figure 12 Steel side of shear fracture of TA1/304 clad plate at 850 °C with a reduction ratio of 35%: (**a**), (**d**) recrystallization of TA1 layer and 304 layer; (**b**), (**e**) statistical results of 304 stainless steel side; (**c**), (**f**) statistical results of TA1 side

plates at 800 °C was caused by interface fracture and TA1 matrix tearing, and EAR increased the proportion of TA1 matrix tearing.

Figure 16 shows the shear fracture morphology of the 304 side under different rolling conditions at 850 °C. When the reduction ratio was 35% under CR conditions, the area of TA1 matrix tearing on the steel side of the shear fracture accounted for approximately half of the entire shear area. The area of TA1 matrix tearing under the EAR condition increased significantly; however, there was still a small amount of interface cracking.

When the reduction ratio was 48%, the fracture section of the CR process showed that the TA1 matrix and the interface fracture were mixed, whereas the TA1 matrix almost completely covered the entire section under the EAR conditions. In general, the coverage area of TA1 matrix on the shear fracture surface of the TA1/304 clad plates at 850 °C was significantly higher than that at 800 °C. Correspondingly, the proportion of interface fractures was significantly reduced, which indicates that the interface bonding strength was improved, and its shear strength is higher than that of the TA1 matrix. The fracture surface expanded along the TA1 matrix. Local interface fracture during the EAR process may be due to different interface forces during the stretching process. In other words, the lap surface rotates at a certain angle during shearing. When the shear force on the lap surface is no longer uniform, the bending of the TA1 side causes an interface fracture.

4 Discussion
4.1 Interface Element Diffusion

Hot-rolling bonding involves close bonding and elemental diffusion between TA1 and 304 stainless steel. Under a strong rolling force, the metal layers on both sides undergo plastic deformation, and many defects, such as dislocations and vacancies, are formed at the interface. These provide channels for the diffusion of alloying elements, and finally form a complete bonding interface.

As shown in Figure 17, the current flows from the 304 stainless steel during the EAR process, accumulates and flows around the contact tip, and is aggregated in this area as a high-density pulse current. It then flows through the TA1 side and into the negative electrode of the power supply. First, the diffusion activation energy of the alloying elements under the action of a pulsed current is reduced. In other words, the electromigration (EM) effect of the pulse current can provide additional power for the diffusion of atoms under high-density conditions (exceeding a certain threshold current). Simultaneously, vacancy defects are generated at the interface, which introduce new diffusion channels in the material [13]. Second, under the action of the EAR, a large number of fine grains generated on the TA1 side at the interface of the plate provide a higher density of grain boundaries (Figure 9d), and a high
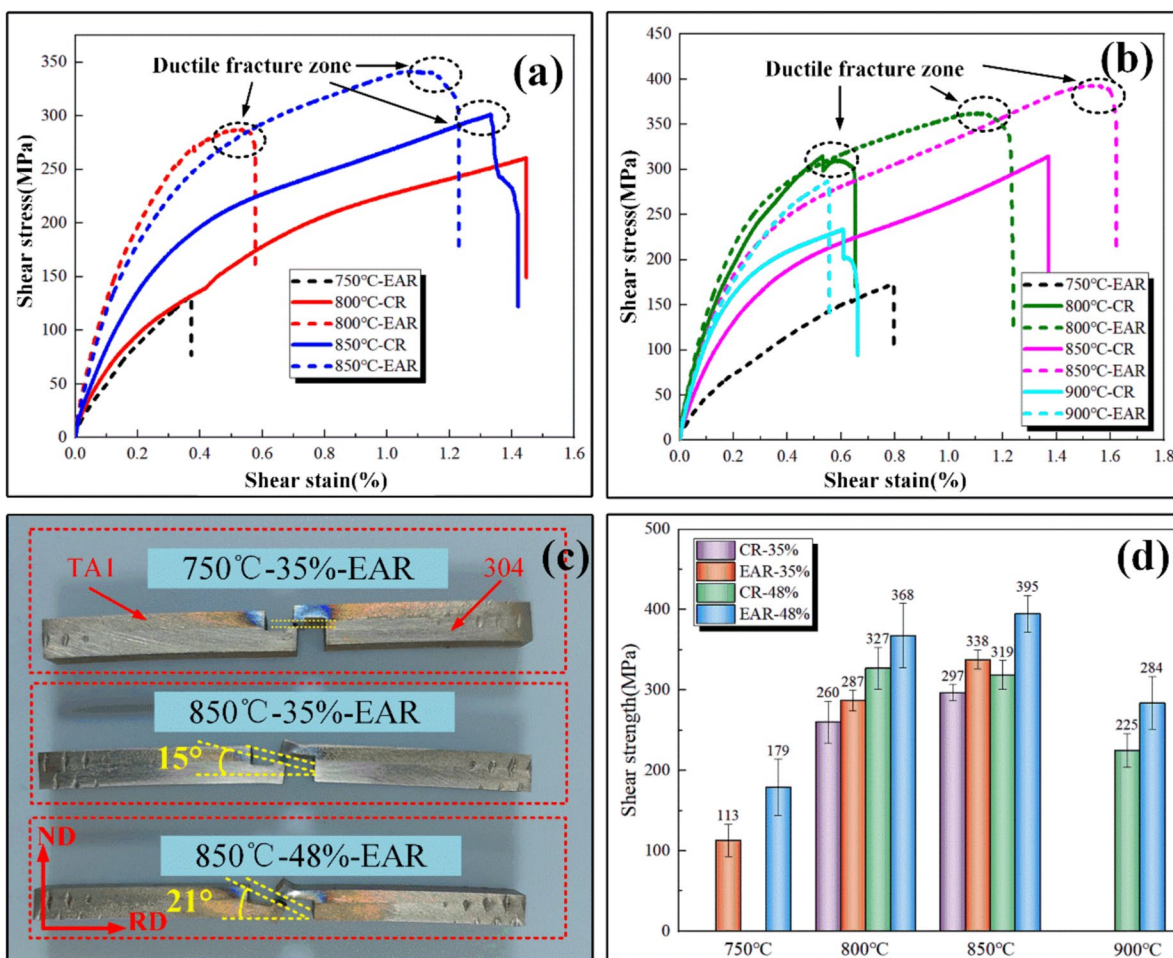
Figure 13 (**a**) Tensile shear strength of TA1/304 clad plates at 35 % reduction ratio, (**b**) Tensile shear strength of TA1/304 clad plates at 48% reduction ratio, (**c**) The profile-view tensile shear fracture characteristics of TA1/304 clad plates at different parameters, (**d**) The profile tensile shear fracture characteristics of TA1/304 clad plates at different parameters

density of dislocations are generated on the steel side (Figure 9f), which produced rich elemental diffusion paths [14]. The increase in the density of structural defects, such as dislocations and vacancies, caused by EAR is beneficial for reducing the diffusion barrier and strengthening the diffusion of elements [15]. However, when the temperature is high, the temperature of the CR is consistent with that of the EAR; the pulse current may have periodic instantaneous effects, and the contribution of the EAR to the element diffusion process is continuous during the high-temperature interface bonding process. Finally, the elemental diffusion distance increases (Figure 4). The element diffusion distance is increased by about 0.3 μm at 800 °C, 35% reduction and 850 °C, 35% reduction. The mutual diffusion of the elements forms a solid-solution diffusion layer at the interface, which strengthens the

interfacial bonding performance and improves the interfacial bonding strength.

Generally, a pulse current can increase the temperature of a metal in a short time. However, in this study, the effect of the pulse current did not lead to an excessive temperature increase at the interface, which can be explained by previous studies. In previous studies, it was reported that complete recrystallization occurred on the TA1 side at 900 °C and a very obvious compound layer formed at 950 °C [16]. However, in this study, no complete recrystallization occurred on the TA1 side (Figure 9d and Figure 12d) and there was no obvious compound layer (Figure 4). This is due to the small range of interface temperature during rolling, which is actually much lower than 900 °C. This can be attributed to the short rolling time and extremely short duration of the pulse current, which was not sufficient to cause a rapid increase in the interface temperature.
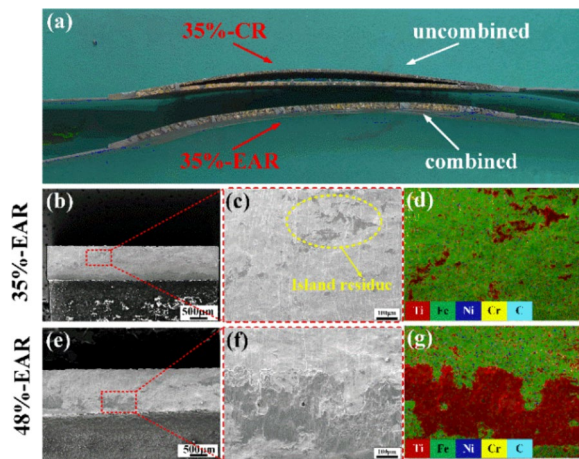
Figure 14 304 side of shear fracture of TA1/304 clad plate at 750℃ with a reduction ratio of 35% and 48%: (**a**) Clad plate photos under different rolling processes; (**b**), (**e**) SEM of shear fracture surface;(**c**), (**f**) Enlarged regions of **b** and **e**; (**d**), (**g**) The element distribution of (**c**) and (**f**)

In other words, the possible influence of the Joule heating effect on the rolling process can be excluded, and it is considered that the strengthening effect of element diffusion mainly depends on the pulse current effect. Therefore, the main reason for the diffusion of elements is the electrical effect of the pulsed current. At 850 ℃, the diffusion distance of elements increases to 2 µm under EAR, which is higher than that of CR.

4.2 Microstructure Evolution

As shown in Figures 7 and 9, the microstructures of the stainless-steel and TA1 matrices after CR and EAR were significantly different. It is well known that the evolution mechanism of grains during rolling is related to the lattice type and stacking fault energy of the material itself.

The stacking fault energy of pure titanium is higher than that of 304 stainless steel [17, 18], and the deformation resistance is lower than that of 304 stainless steel; pure titanium is easier to deform, and dislocations proliferate during rolling. Therefore, as shown in Figure 9

Figure 15 304 side of shear fracture of TA1/304 clad plate at 800 ℃ with a reduction ratio of 35% and 48%: (**a**), (**d**), (**g**), (**j**) SEM of shear fracture surface; (**b**), (**e**), (**h**), (**k**) Enlarged regions of (**a**), (**d**), (**g**) and (**j**); (**c**), (**f**), (**i**), (**l**) the element distribution of (**b**), (), (**h**) and (**k**)

Guo *et al. Chinese Journal of Mechanical Engineering*　　(2024) 37:116
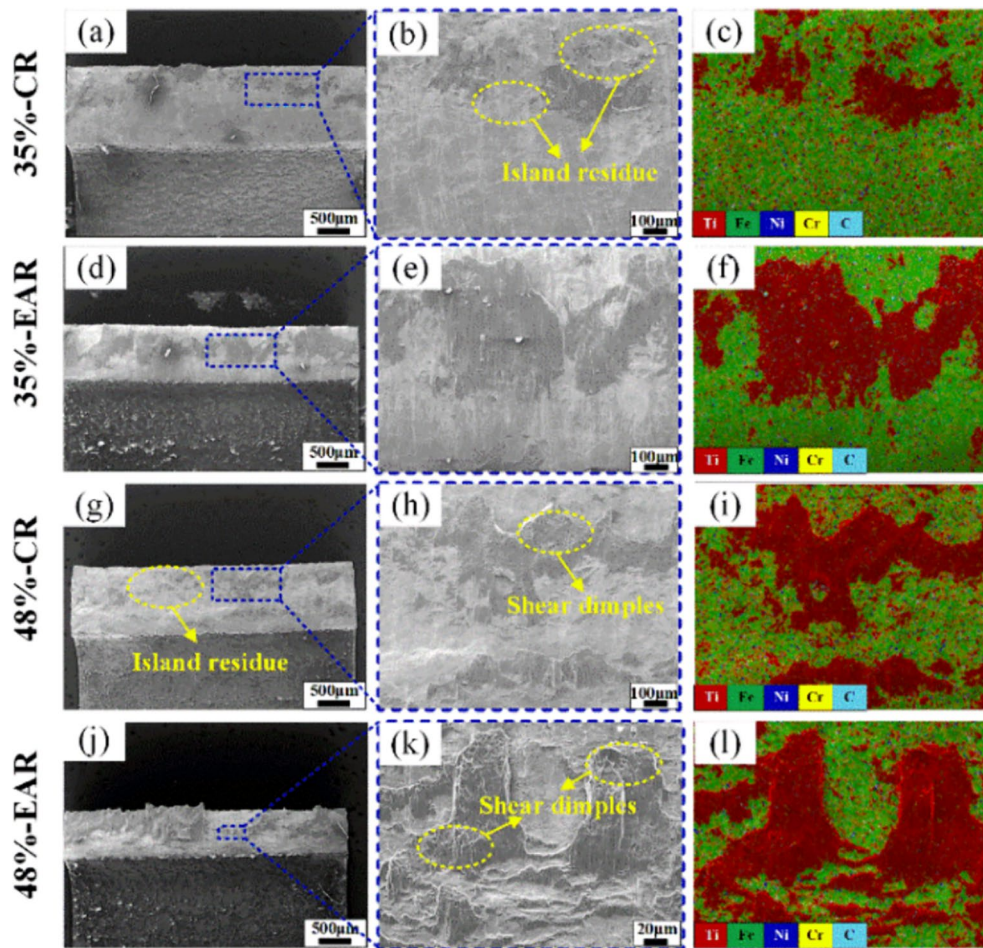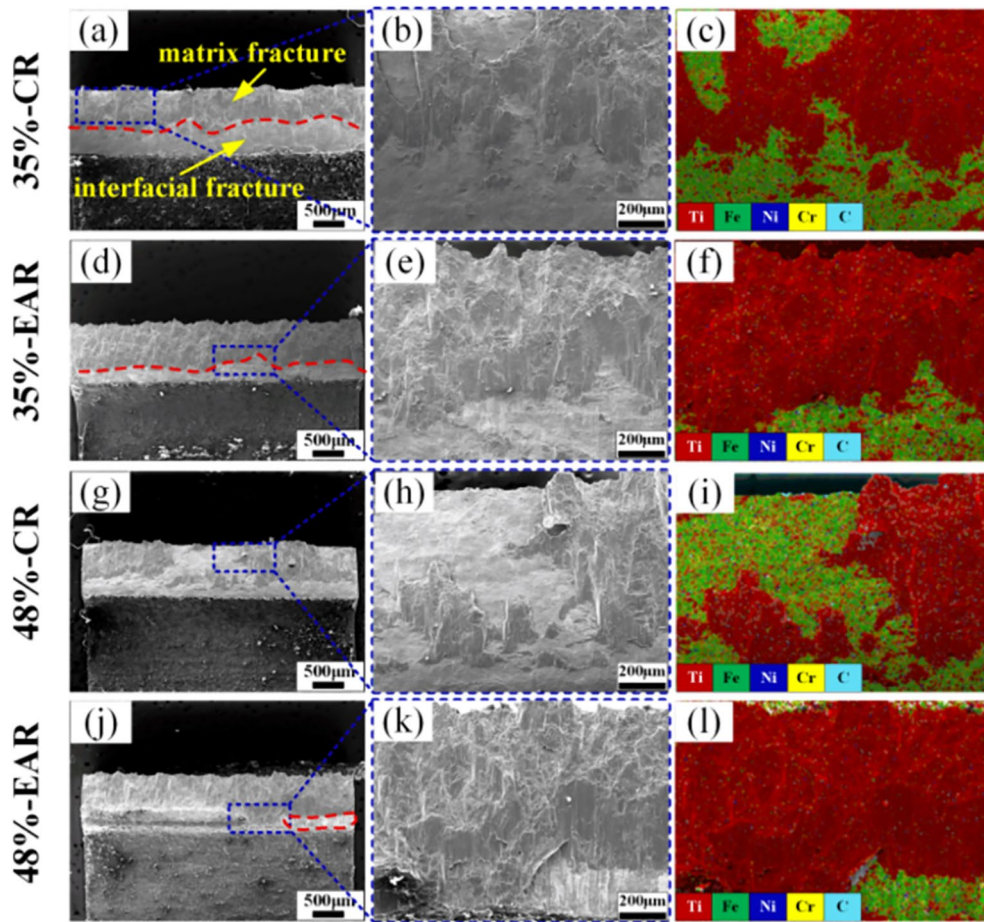
Page 12 of 16

Figure 16 304 side of shear fracture of TA1/304 clad plate at 850°C with a reduction ratio of 35% and 48%: (**a**), (**d**), (**g**), (**j**) SEM of shear fracture surface; (**b**), (**e**), (**h**), (**k**) enlarged regions of **a**, **d**, **g** and **j**; (**c**), (**f**), (**i**), (**l**) the element distribution of (**b**), (**e**), (**h**) and (**k**)
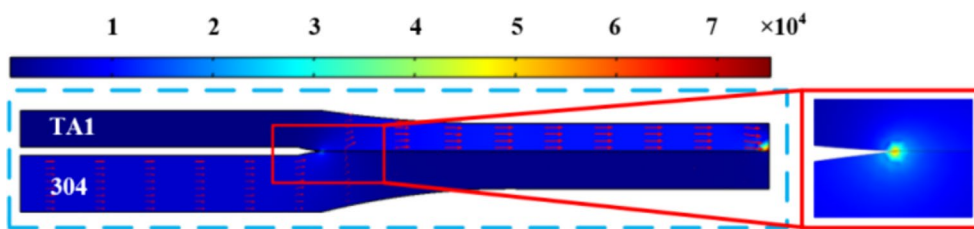

Figure 17 Current density distribution of rolling process

and Figure 11, the GND density on the TA1 side is 5.41 × 1014 m^{-2}, which is higher than that on the stainless-steel side (4.94 × 1014 m^{-2}). During the EAR, a high-density pulse current was collected at the interface, the TA1 matrix softened, and a stronger shear force was received during the rolling deformation process. This shear force contributed to the proliferation and slip of dislocations in the titanium crystals. At the same time, the pulse current helped the subgrain structure in the

TA1 grains break through the energy barrier to form grain boundaries, promote the rotation and refinement of the grains, transform the LAGBs into HAGBs, and lead to the formation of shear bands on the TA1 matrix side (Figure 9d).

For 304 stainless steel, the size and proportion of LAGBs in the matrix gradually increased (Figure 7), and the average grain boundary misorientation decreased (Figure 8) after the EAR. This is due to the friction
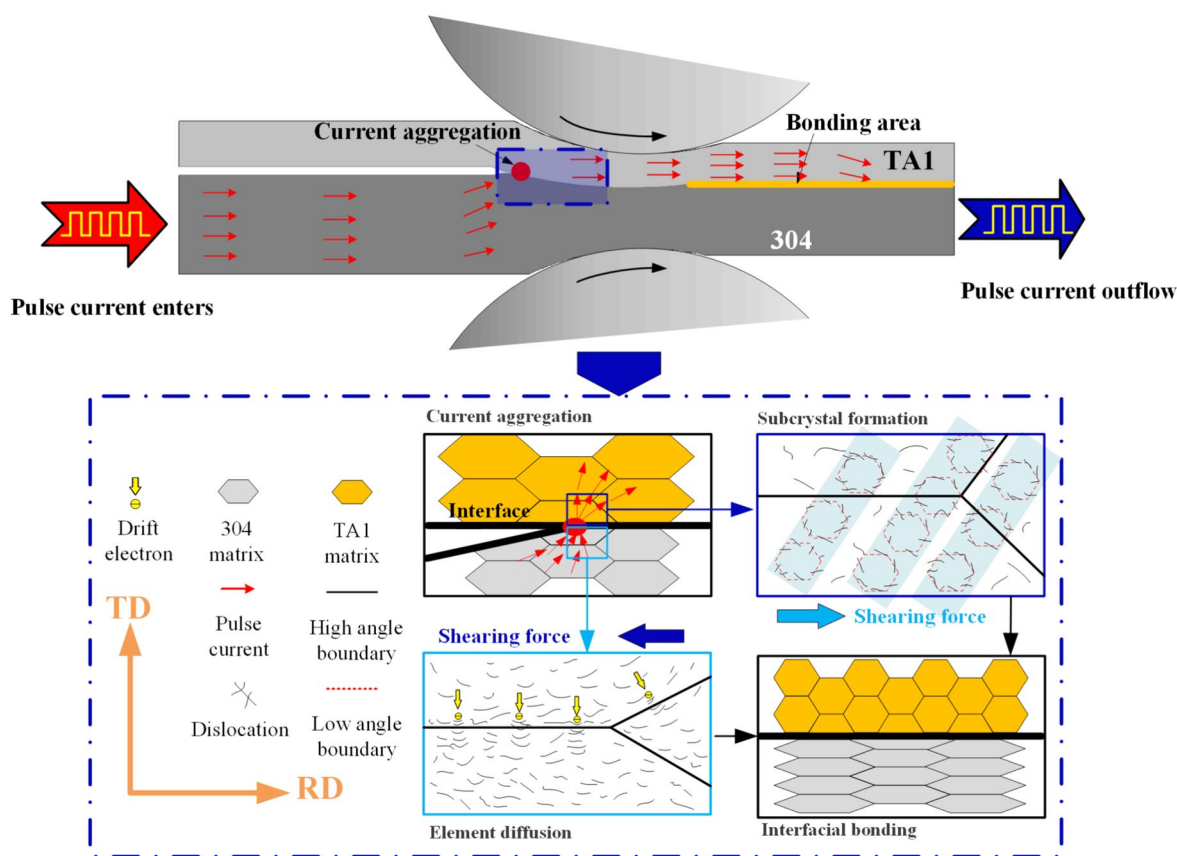
Figure 18 Microstructure change mechanism of rolling process

between the bimetal contact surfaces during CR, as well as the shear force being the largest near the interface, while a larger plastic deformation is produced and the dislocation density increases (Figure 9 c). Away from the interface, there was a high dislocation density near the grain boundary, and the dislocation density inside the grains was low. This is due to the hindrance of the grain boundaries due to dislocations. Dislocations accumulate at the grain boundaries adjacent to the interface [19], making it difficult for them to cross and continue to transfer downward. During EAR, the pulsed current helped the dislocations move, forming a higher dislocation density in the grains far from the interface (Figure 9f). As 304 stainless steel softens under a high-density current, the grains were elongated under rolling pressure, and deformation accumulated near the interface, but this did not lead to obvious grain refinement. It can be clearly seen from Figure 12 that the proportion of deformed crystals on the side of 304 stainless steel after EAR increased significantly, which again shows that the deformation degree of 304 stainless steel increased after EAR.

Based on the above analysis, the micro-texture evolution of the TA1/304 stainless-steel clad plates during EAR is summarized and schematically shown in Figure 18. It mainly includes four stages: current accumulation occurs at the tip of the area to be bonded at the beginning of rolling, the interface matrices squeeze each other during the rolling process to produce large plastic deformation, interface bonding, and the diffusion of interface elements accelerates under the action of the current. During the rolling process, the high-density pulse current gathered in the transition region between the bonded and unbonded regions led to a decrease in the deformation difference between the matrix and the interface (Figure 7). The strain distribution extended from the middle region concentrated in the thickness direction of the matrix to the entire thickness direction, that is, homogenization. The higher the temperature, the more significant the phenomenon. This implies that for the same overall strain, the reduction ratio is consistent with the thickness ratio, and the metal matrix near the interface undergoes a greater plastic deformation under the action of the rolling force. At this time, the strong shear stress at the interface leads to

the tearing of the metal surface, which causes the new metal to be squeezed into the opposite matrix, thereby further enhancing interface bonding. TA1 underwent dislocation proliferation and grain refinement under the action of a strong shear force, whereas stainless steel extended along the rolling direction under the action of the interface friction shear force. The grains were elongated, and dislocations proliferated inside the grains. Under the action of the pulse current, the dislocation movement accelerated and proliferated inside the grains far from the interface, while under the action of high-density dislocations and current, element diffusion and interface bonding are further strengthened. Therefore, the pulse current played a key role in the change in the microstructure of the composite plate matrix and the increase in the dislocation density, which is not possible in CR.

4.3 Shear Strengthening Mechanism

The microstructure of a material significantly affects its mechanical properties [20]. The results in Figure 9 show that significant grain refinement occurred near the interface of the TA1 matrix, and the fine-grained strengthening effect was evident. The form of shear fracture was directly related to the state of the near-interface matrix on the TA1 side. At the same time, the stress change during the tension-shear process also caused the near-interface matrix to participate in shear deformation to a greater extent. Therefore, fine-grained strengthening was manifested in the subsequent shear properties.

The shear fracture process primarily includes interface fracture and matrix tearing. As shown in Figure 13c, different shear strengths lead to different angles between the fracture surface and rolling direction. In this study, the shear strength was the highest at 850 °C-48%-EAR, and the torsion angle of the corresponding fracture was the largest, reaching 21°. The shear strength at 750°C-35%-EAR is only 113 MPa, and the fracture had almost no torsion. Liu et al. [21] reported similar phenomena after shear tests on stainless-steel clad plates at different degrees of vacuum. Studies have shown that an increased torsion angle indicates increased bonding strength. To further study the reason for this phenomenon, Wu et al. [16] observed the microstructure of the TA1 matrix under varied working conditions and found that the matrix dislocation density, recrystallization degree, and element diffusion degree differed under different working conditions, which led to a difference in the TA1 matrix strength, and the difference was reflected in the shear strength. At 750 °C, the CR process cannot successfully bond the clad plate (Figure 14a). Although the EAR

can successfully bond a clad plate, its bonding strength is not high. When the reduction ratio was 35%, only a very small amount of TA1 matrix residue was bonded to the steel side of the shear fracture surface, and the shear strength was only 113 MPa. When the reduction ratio is increased to 48%, the TA1 matrix residue on the shear section increased significantly, but the shear strength was still not greatly improved.

At 800 °C and 850 °C, the interface shear strength was related to the amount of TA1 bonding, and a greater amount of bonding led to a higher shear strength. At 800 °C, the shear fracture generally showed a mixed fracture morphology of interface fracture and TA1 matrix tearing, and the proportion of TA1 matrix tearing was not high. At 850 °C, the tearing ratio of the TA1 matrix in the shear section increased significantly. Under CR conditions, the tearing of TA1 matrix accounted for approximately 50% of the entire shear section. Under EAR conditions, the shear fracture surface was almost full of the TA1 matrix, indicating that the interface bonding strength exceeded the strength of the TA1 matrix. According to GB / T 3280-2015 [22], the tensile strength of 304 stainless steel matrix is not less than 520 MPa. According to GB / T 3621-2007 [23], the tensile strength of TA1 is not less than 240 MPa. The matrix strength of 304 stainless steel is much larger than that of TA1; therefore, it is reasonable for shear fracture to occur on the TA1 side. Additionally, due to the large number of dislocations and work hardening in the TA1 matrix after rolling, the strength of the matrix will be improved, and the shear strength of the clad plate will be as high as 395 MPa. The reason for the decrease of bonding strength at 900 °C is the matrix softening caused by the recrystallization growth of TA1, as seen in previous studies [16].

The SEM images of the shear fracture surfaces in Figures 14, 15, 16 show that when the shear strength is high, the area ratio of the shear fracture at the interface is very small. This is because the diffusion of elements under the action of the pulsed current was enhanced, which contributed to the enhancement of interface bonding. The ability of the interface to withstand shear was greater than that of the TA1 matrix; therefore, fractures occurred on the TA1 matrix side. Simultaneously, it is necessary to consider that the interface is no longer simply subjected to shear after torsion during the shear process and that the interface position will be subjected to the combined action of tensile and shear forces. A clad plate with a low interface bonding strength is more likely to crack at the interface during the shear process. This phenomenon gradually improves with an increase in bonding strength, indicating that the clad plate has a better ability to withstand shear force. Overall, the interface cracking area under the EAR condition was smaller than that under

Guo *et al. Chinese Journal of Mechanical Engineering*   (2024) 37:116

Page 15 of 16

the CR condition, indicating that the interface of the clad plate prepared using EAR can withstand a higher shear force and have a higher bonding strength.

5 Conclusions

(1) EAR promotes the diffusion of elements at the interface of the TA1/304 clad plates, which can make the interface form a stronger combination. Under EAR (500 A, 1500 Hz, 50 duty cycle), the clad plates can be initially bonded at 750 °C and a 35 % reduction ratio, which cannot be achieved by CR. Finally, the diffusion distance of interface elements reached 2 μm at 850 °C -EAR-48%.

(2) After EAR, shear bands and a large number of fine grains were formed on the titanium side of the clad plate, and dislocations with high density and uniform distribution were formed on the steel side, which had a positive effect on the element diffusion and shear strength of the clad plate.

(3) The TA1/304 clad plates prepared by the EAR process had higher shear strength and shear resistance in the case of uneven shear stress. When processing with EAR at 850 °C, the shear strength reached 338 MPa and 395 MPa under 35 % and 48 % reduction, respectively. Shear fracture occurred on the TA1 matrix side.

Author Contributions
XG was in charge of the experimental process and writing the manuscript; ZR and PZ was in charge of simulation and assisting the experiment; CZ, SJ and QZ were in charge of pictures and some manuscripts; TW and QH were in charge of review and editing. All authors read and approved the final manuscript.

Data availability
Data will be made available on request.

Declarations

Competing Interests
The authors declare no competing financial interests.

References
[1] C Yu, Z C Qi, H Yu, et al. Microstructural and mechanical properties of hot roll bonded titanium alloy/low carbon steel plate. *Journal of Materials Engineering and Performance*, 2018, 27(3): 1-9.
[2] Z P Zhao, N ul H Tariq, J Tang, et al. Microstructural evolutions and mechanical characteristics of Ti/steel clad plates fabricated through cold spray additive manufacturing followed by hot-rolling and annealing. *Materials and Design*, 2022, 185: 108249.
[3] C Yu, H Xiao, N Li, et al. Effect of DT4 interlayer on properties of hot-roll bonding TA2/Q235B plate. *IOP Conference Series: Materials Science and Engineering*, 2017, 229: 012017.
[4] B Qin, G M Sheng, J W Huang, et al. Phase transformation diffusion bonding of titanium alloy with stainless steel. *Materials Characterization,* 2006, 56(1): 32-38.
[5] Z H Xu, G Y Tang, S Q Tian, et al. Research of electroplastic rolling of AZ31 Mg alloy strip. *Journal of Materials Processing Technology*, 2007, 182: 128-133.
[6] J Kuang, T S E Low, S R Niezgoda, et al. Abnormal texture development in magnesium alloy Mg-3Al-1Zn during large strain electroplastic rolling: Effect of pulsed electric current. *International Journal of Plasticity,* 2016, 87: 86-99.
[7] X W Guo, Z K Ren, X B Ma, et al. Effect of temperature and reduction ratio on the interface bonding properties of TC4/304 plates manufactured by EA rolling. *Journal of Manufacturing Processes*, 2021, 64: 664-673.
[8] T T Zhang, Y Wang, Z B Xu, et al. A new method for fabricating Mg/Al alloy composites by pulse current-assisted rolled welding. *Materials Letters*, 2023, 330: 133247.
[9] Z K Ren, X W Guo, X Liu, et al. Effect of pulse current treatment on interface structure and mechanical behavior of TA1/304 clad plates. *Materials Science and Engineering: A*, 2022, 850: 143583.
[10] W Zhao, R F Liu, J Yan, et al. Overall optimization in microstructure and mechanical properties of 5 wt% SiC/7075Al composites by high-frequency electric pulse assisted treatment. *Journal of Materials Research and Technology*, 2022, 21: 2156-2167.
[11] H Gao, Y Huang, W D Nix, et al. Mechanism-based strain gradient plasticity - I. Theory. *Journal of the Mechanics and Physics of Solids*, 1999, 47(6): 1239-1263.
[12] L P Kubin, A Mortensen. Geometrically necessary dislocations and strain-gradient plasticity: A few critical issues. *Scripta Materialia*, 2003, 48(2): 119-125.
[13] F C Shen, C Y Huang, H Y Lo, et al. Atomic-scale investigation of electromigration with different directions of electron flow into high-density nanotwinned copper through in situ HRTEM. *Acta Materialia,* 2021, 219: 117250.
[14] Y N Chen, S S Liu, Y Q Zhao, et al. Diffusion behavior and mechanical properties of Cu/Ni coating on TC4 alloy. *Vacuum*, 2017, 143: 150-157.
[15] L J Wirth, A A Farajian, C Woodward. Density functional study of self-diffusion along an isolated screw dislocation in FCC Ni. *Physical Review Materials*, 2019, 3: 033605.
[16] Y Wu, T Wang, Z K Ren, et al. Evolution mechanism of microstructure and bond strength based on interface diffusion and IMCs of Ti/steel clad plates fabricated by double-layered hot rolling. *Journal of Materials Processing Technology*, 2022, 310: 117780.
[17] Y F Shen, X X Li, X Sun, et al. Twinning and martensite in a 304 austenitic stainless steel. *Materials Science and Engineering: A*, 2012, 552: 514-522.
[18] Z Guo, A P Miodownik, N Saunders, et al. Influence of stacking-fault energy on high temperature creep of alpha titanium alloys. *Scripta Materialia*, 2006, 54(12): 2175-2178.
[19] J H Xu, L Huang, Y K Xu, et al. Effect of pulsed electromagnetic field treatment on dislocation evolution and subsequent artificial aging behavior of 2195 Al-Li alloy. *Materials Characterization*, 2022, 187: 111872.

[20] K Chen, L H Zhan, Y Q Xu, et al. Effect of pulsed current density on creep-aging behavior and microstructure of AA7150 aluminum alloy. *Journal of Materials Research and Technology*, 2020, 9(6): 15433-15441.

[21] B X Liu, S Wang, C X Chen, et al. Interface characteristics and fracture behavior of hot rolled stainless steel clad plates with different vacuum degrees. *Applied Surface Science,* 2019, 463: 121-131.

[22] General Administration of Quality Supervision, Inspection and Quarantine of the People's Republic of China, Standardization Administration of the People's Republic of China. GB/T 3280—2015 Cold rolled stainless steel plate, sheet and strip. Beijing: China Standard Publishing House, 2015. (in Chinese)

[23] General Administration of Quality Supervision, Inspection and Quarantine of the People's Republic of China; Standardization Administration of the People's Republic of China. GB/T 3621—2007 Titanium and titanium alloy plate and sheet. Beijing: China Standard Publishing House, 2007. (in Chinese)

Xiongwei Guo born in 1994, is currently a PhD candidate at *College of Mechanical and Vehicle Engineering, Taiyuan University of Technology, China.*

Zhongkai Ren born in 1988, is currently an associate researcher and a master instructor at *Engineering Research Center of Advanced Metal Composites Forming Technology and Equipment of Ministry of Education, Taiyuan University of Technology, China.*

Pengjie Zhang born in 1998, is currently a master candidate at *College of Mechanical and Vehicle Engineering, Taiyuan University of Technology, China.*

Chao Zhang born in 1997, is currently a master candidate at *College of Mechanical and Vehicle Engineering, Taiyuan University of Technology, China.*

Shuyong Jiang born in 1973, is currently a professor and a PhD candidate supervisor at *Engineering Research Center of Advanced Metal Composites Forming Technology and Equipment of Ministry of Education, Taiyuan University of Technology, China.*

Qi Zhang born in 1988, is currently a lecturer at *Engineering Research Center of Advanced Metal Composites Forming Technology and Equipment of Ministry of Education, Taiyuan University of Technology, China.*

Tao Wang born in 1985, is currently a professor and a PhD candidate supervisor at *Engineering Research Center of Advanced Metal Composites Forming Technology and Equipment of Ministry of Education, Taiyuan University of Technology, China.*

Qingxue Huang born in 1960, is currently a professor and a PhD candidate supervisor at *Engineering Research Center of Advanced Metal Composites Forming Technology and Equipment of Ministry of Education, Taiyuan University of Technology, China.*